Indian Journal of Chemical Technology
Vol. 33, May 2026, pp. 427-443
DOI: 10.56042/ijct.v33i3.15734

Influence of injection strategy and combustion chamber geometry on the performance and emissions of a bio-ethanol fuelled CRDI diesel engine

Tamilarasan Velliyampalayam Devaraj[1]*, Ramesh Kumar Thiruppathi[2] & Arivazhagan Sampathkumar[3]

[1]Department of Automobile Engineering, Dr. Mahalingam College of Engineering and Technology, Coimbatore, Tamil Nadu, India

[2]Department of Mechanical Engineering, Bannari Amman Institute of Technology, Erode, Tamil Nadu, India

[3]Department of Mechanical Engineering, Sri Krishna College of Technology, Coimbatore, Tamil Nadu, India

*E-mail: tamil.maritime@gmail.com

Received 15 December 2024; accepted 2 March 2026

Owing to the growing depletion of fossil fuels and increasing environmental impacts, alternative fuels such as bio-ethanol are becoming more attractive for use in compression ignition (CI) engine. The current study examines the impact of combustion chamber geometry and injection pressure on improving performance, reducing emissions, and enhancing combustion characteristics in a bio-ethanol fuelled diesel engine. Experimental tests were performed using bio-ethanol fuel (EPMD85: 85 % Ethanol, 7% PEG, 4% MTBE & 4% DEE), in a common rail direct injection (CRDI) diesel engine. Hemispherical (HCC) and Toroidal re-entrant (TRCC-B) combustion chamber geometries have been evaluated at a compression ratio (CR) of 28.5:1 and injection pressure (IP) of 1200 bar. The results indicate that the brake thermal efficiency for EPMD85-TRCC-B (28.5:1, 1200 bar) is higher than EPMD85-HCC (28.5:1, 1200 bar) and ultra-low sulfur diesel (ULSD)-HCC (17.5:1, 220 bar), although ULSD-HCC exhibits lower specific fuel consumption (SFC) than EPMD85-TRCC-B and EPMD85-HCC. EPMD85-TRCC-B achieves substantial reduction in nitrogen oxide (NOx), carbon monoxide (CO), unburnt hydrocarbon (UBHC), carbon dioxide (CO_2) and smoke compared to EPMD85-HCC and ULSD-HCC. Furthermore, the experimental results are compared with Diesel-RK simulation data under same operating condition, confirming that the EPMD85-TRCC-B combustion chamber at an IP of 1200 bar provides improved performance and enhanced combustion and reduced emissions.

Keywords: Bio-ethanol, CRDI, Combustion chamber geometry, Emission, Injection pressure

Introduction

Intense competition and worldwide pollution regulations have placed unprecedented expectations on performance and emission of current internal combustion (IC) engines. Over the last few decades, energy conservation and emission have grown increasingly crucial due to increasing vehicle usage and establishment of new industries have resulted in the fuel crisis. The quality of air is tremendously affected by increased automobile emissions, including carbon monoxide (CO), carbon dioxide (CO_2), unburnt hydrocarbons (UBHC), particulate matter (PM), nitrogen oxide (NO_x) and smoke[1,2]. Hence, there has been increased interest in biofuels such as alcoholic fuels (methanol, ethanol, butanol etc.) and vegetable oils (Jatropha, soybean, algae oil etc.) are rapidly getting advanced for use in modern CI engines[3-8].

Biodiesel, alcohol-based fuels and ether fuels have gained increasing attention in recent years owing to their abundant availability and potential for local production. Additionally, it may be mixed with hydrocarbon fuels to enhance energy efficiency and environmental advantages. Several studies revealed that using pure vegetable oil/biodiesel/alcohol as a fuel in the engine resulted in problems such as cold starting problem, injector surface coking, carbon deposition in piston head and rings, and abnormal combustion[9]. Alcoholic fuels (methanol, ethanol, and n-butanol), which may have been blended with diesel fuel, have greater fuel properties than vegetable oil. Bio-ethanol is a sustainable fuel that is made by fermentation of agriculture feedstock such as sugar beet, wheat, corn, and sugar cane[10]. Sakthivel *et al.*[11] investigated attributes of ethanol, including its higher octane number, low viscosity, high self-ignition temperature, and high enthalpy of vaporization. Despite these characteristics, pure ethanol cannot be directly utilized as fuel for CI engines. However, it was found that blending alcohol with diesel improved brake thermal efficiency (BTE) and decreased CO, UBHC, and NO_x emissions. Lei *et al.*[12] examined the

impact of diesel-ethanol blends ranging from 10% to 40% in diesel engines under experimental conditions. The results revealed that increasing the fuel blend ratio and load led to higher brake specific fuel consumption (BSFC), as well as higher emissions, including UBHC and CO.

Currently, diesel engines are unable to operate effectively with ethanol-diesel blend / neat bio-ethanol as fuel owing to combustion limitation. The performance and emission characteristics of diesel engines are significantly affected by a variety of factors, including fuel properties, combustion chamber geometry, fuel injection parameters, air momentum, fuel spray pattern, compression ratio (CR), and air-fuel ratio[13,14]. To address these issues, the researchers intend to implement four deliberate strategies to enhance the combustion and performance of the identified bio-ethanol blended fuel. These strategies include using special additives, varying compression ratio, modifying combustion chamber geometry and injection pressure.

Combustion is a complex process wherein engine performance and emissions are potentially influenced by many parameters. Alcoholic fuels are being investigated as fuel additives for compression ignition (CI) engines. Due to their higher octane ratings, these may be utilized as an alternate fuel for spark-ignition (SI) engines[15]. Furthermore, prior research reveals that without adding any special additives, diesel engines cannot run normally on ethanol–diesel blends[13,16-19]. Ali Turkcan[20] and Guo *et al*.[21] conducted an extensive analysis of the fuel mixtures with lower cetane number, which delayed the initiation of combustion, resulting in abnormal combustion and increased exhaust emission from CI engine. Among the several biofuels, oxygenated fuel is a feasible option for CI engine[22]. Oxygenated fuel additives, such as Dimethyl ether (DME), methyl tertiary butyl ether (MTBE), dibutyl ether (DBE), dimethyl carbonate (DMC), diethyl ether (DEE) and polyethylene glycol (PEG) have contributed to improving the specific properties of diesel fuel/diesel-bioethanol blend/biodiesel/bio-ethanol, bringing them closer to diesel fuel characteristics[23-25]. PEG, MTBE, and DEE are oxygenated fuels with higher cetane numbers than diesel fuel and greater calorific values than ethanol and butanol[26-29]. It has been found that, without modifications to the diesel engine, DEE cannot be used as the sole sustainable fuel, adding up to 20% DEE to diesel fuel increased engine BTE and NO_x emissions while reducing smoke, CO, and UBHC emissions[30]. Venu and Madhavan[31] discovered that adding 5% DEE to ternary blends improved combustion and emission reduction compared to adding 10% DEE. Research on ethanol-biodiesel-diesel (EBD) and methanol-biodiesel-diesel (MBD) blends showed that incorporating DEE additives led to reductions in ignition delay (ID), particulate matter (PM), and smoke. MTBE possess a low breaking point, high cetane number, and high oxygen content makes it an attractive oxygenated additive and a suitable ignition improver for IC engines. Due to its high viscosity, PEG lubricates engine components, prolonging their lifetime[32]. Sivakumar *et al*.[33] investigated the impact of MTBE blended diesel fuel on CI engine to enhance BTE and minimize UBHC, CO, and smoke emissions. Simonsen & Chomiak[25] experimentally studied that nitrate-based ignition improvers resulted in shorter ignition times but higher NO_x emissions compared to PEG improvers. In comparison with diesel fuel, the authors reported that the cetane number of ethanol increased to approximately 44 with the addition of 4% nitrate-based cetane improvers, while a cetane number of about 40 was achieved when 7% PEG was used. Savo Gjirja & Olsson[34] recommended 7% by weight of PEG ignition improver in ethanol for high-compression ignition engines to enhance combustion and ignition delay.

Combustion chamber geometry plays a significant role in air-fuel mixture and can be effectively adaptable for alternative fuels. For conventional diesel fuel, the standard hemispherical combustion chamber improves combustion efficiency and higher emissions. Premnath and Devaradjane[35] experimentally studied the effect of injection pressure and combustion chamber geometry, finding that a modified re-entrant combustion chamber (RCC) reduced harmful emissions such as UBHC, NO_x, CO and smoke. Gafoor and Gupta[36] investigated a combustion chamber geometry for quick atomization of air and fuel mixture. They observed that the swirl ratio significantly influenced ignition delay, and that increased injection pressure and decreased injector nozzle diameter resulted in shorter ignition delays. Mamilla *et al*.[37] examined the impact of a toroidal re-entrant combustion chamber (TRCC) in comparison to spherical (SCC) and toroidal (TCC) combustion chambers using 20% Jatropha methyl esters in CI engine. In comparison to SCC and TCC, they discovered that TRCC improved performance while decreasing emissions of HC, CO and smoke. Jaichandar and Annamalai[38] observed that TRCC geometries increased in-cylinder air motion, squish,

swirl, and air-fuel atomization rates compared to HCC geometries. Consequently, improvements were noted in BTE, in-cylinder pressure (ICP) and heat release rate (HRR), whereas reductions were observed in BSFC, ID, CO, UBHC, and smoke emissions.

Injection parameters are another technique for improving combustion and increasing engine performance with alternative fuels. Injection time (IT) and pressure (IP) directly influence fuel atomisation, vaporisation, dispersion, and droplet mean diameter. Jaichandar *et al.*[14] observed that lowering engine speed and load while increasing injection pressure resulted in improved atomization and a well-mixed fuel-to-air ratio, leading to complete combustion. Cenk Sayin *et al.*[39] noted that variation in IP and IT resulted in a decrease in smoke opacity, CO and UBHC, along with an increase in NO_x. Jiaqiang *et al.*[40] experimentally evaluated the impact of fuel injection pressure using fish oil biodiesel. The researchers found that adding biodiesel to diesel fuel reduced BTE, it increased UBHC, CO and NO_x emissions from diesel fuel. Raheman *et al.*[41] experimentally studied the effect of CR and IP in a Richard E6 engine using mahua oil and its blend. This study revealed that increasing the compression ratio (CR) from 18 to 20 resulted in a 38% increase in BTE, probably due to a shorter ignition delay time.

The present research investigates the combined effect of combustion chamber geometry, compression ratio (CR), and injection pressure (IP) on the performance, combustion, and emissions of a CRDI single-cylinder CI engine using bio-ethanol with additives. The literature reveals a clear gap regarding the application of high percentage bio-ethanol blend like EPMD85 (Bio-ethanol-85%, Polyethylene glycol-7%, Methyl-tetra butyl ether-4% and Di-ethyl ether-4%) in diesel engine, which necessitates modifications in combustion chamber geometry, CR, and IP. Furthermore, the effect of EPMD85 fuel on diesel engine characteristics are examined using Diesel-RK thermodynamic simulation tool and validated against experimental results. Fig. 1 illustrates the problem statement and also the objective of the current investigation.

Experimental Section

Biofuel synthesis and properties

In the current investigation, pure bio-ethanol with 99.9% purity was employed as an alternative for a CI engine, along with fuel additives such as poly ethylene glycol (PEG), methyl tetra butyl ether (MTBE) and diethyl ether (DEE) to enhance the certain properties of bio-ethanol. The bio-ethanol and fuel additives were purchased from Modern Scientific Co. and Ponmani & Co., Coimbatore, Tamil Nadu, India. The preparation of test fuel and the testing were performed in the Fuel and lubrication laboratory, Department of Mechanical Engineering, Bannari Amman Institute of Technology, Sathymangalam. Based on the literature review and testing of different fuel bends, the (EPMD85) 85% bio-ethanol was blended with fuel additives at 7% PEG, 4% MTBE and 4% DEE by volume and used as fuel for this current research[19,24,43]. As MTBE and DEE are high volatile in nature and PEG has good lubricating properties, after addition of MTBE, DEE and PEG with bio-ethanol, the blends were taken into closed container and blends were shaken for 15 min using a mechanical shaker machine. The stability was evaluated using a centrifuge at 3000 rpm at an ambient temperature of approximately 25°C for 15-20 min and followed by physical observation for 10 days. The empirical formula used to compute the cetane number of the test blend is as follows[44]

$$CN_{epmd\,85} = (CN_{be} * \omega_{be}) + (CN_{peg} * \omega_{peg}) + (CN_{mtbe} * \omega_{mtbe}) +) + (CN_{dee} * \omega_{dee}) \quad \ldots(1)$$

Fig. 1 — A graphical illustration of the research objectives and problem statement

where $CN_{epmd\,85}$ is the cetane number of test fuel EPMD85 blend; CN_{be}, CN_{peg}, CN_{mtbe} and CN_{dee} are the cetane numbers of bio-ethanol, PEG, MTBE and DEE respectively and ω_{be}, ω_{peg}, ω_{mtbe} and ω_{dee} are the fractional content of bio-ethanol, PEG, MTBE and DEE in the blend. The fuel property measurements and engine performance tests were conducted at an ambient temperature of 25-30°C, which is below the boiling point of bio-ethanol, MTBE and DEE[45,46]. To determine the impact of the additives, the EPMD85 blend was tested in an existing engine. The main fuel properties provided in Table 1 and the blend is illustrated in Fig. 1. The fuel characteristics of EPMD85, including density, viscosity, flash point, calorific value, cetane number, cloud point, pour point and copper strip corrosion, were measured as per American Society for Testing and Materials (ASTM) standard, as indicated in Table 1.

Experimental setup and specifications

This investigation was performed in a CRDI assisted Kirloskar TV 1 model, 4-stroke, single cylinder, water-cooled, CI engine. For loading operation, an eddy current dynamometer (Technomech, Model-TMEC10) was employed to synchronize the engine. The schematic layout for the engine test rig configuration is illustrated in Fig. 2 and the technical specifications are shown in Table 2. The crankshaft was loaded on an eddy current dynamometer cooled by water, using electromagnetic force controlled by the load cell (Sensotronics sanmar Ltd, Model-60001). With the help of a burette setup and a stopwatch, the time necessary for 100cc of fuel consumption is recorded. A piezoelectric transducer (PCB piezoelectric, Model-S111A22) was employed to measure both the in-cylinder as well as the fuel line pressure.An optical encoder (Kubler, Model 8.KIS40.1361.0360 Clamping/Synchro flange) mounted on the flywheel was employed to measure

Table 1 — Properties of ULSD, Bio-Ethanol, Polyethylene glycol, Methyl tertiary butyl ether, Diethyl ether and its blending stocks

Properties	ULSD	BIO-ETHANOL	PEG	MTBE	DEE	EPMD85	Test method IS1448/ASTM
Molecular weight (g/mol)	226.4	46.07	200	88.15	74.12	59.65	ASTM D86
Density (kg/m^3) at 20°C	850	789	1128	740	713	805.3	ASTM D1298
Calorific value (kJ/kg)	44189	28843	22460	35110	36840	29744	ASTM D240
Kinematic viscosity (cSt) at 25°C	2.9	1.2	52	0.36	0.244	3.24	ASTM D445
Flash point (°C)	56	17	185	-28	-40	41	ASTM D93
Cloud point (°C)	-8.6	-6	-8	-6	-15.5	-6.5	ASTM D2500
Pour point (°C)	-15	-8	-28	-30	-21	-11	ASTM D97
Copper strip corrosion test 3hr at 100 °C	1a	1a	1a	1a	1a	1a	ASTM D130
Carbon residue (% mass)	0.12	0.021	0.019	0.024	0.015	0.018	ASTM D189
Cetane number	51.6	12	412	8.50	125	46.38	ASTM D613

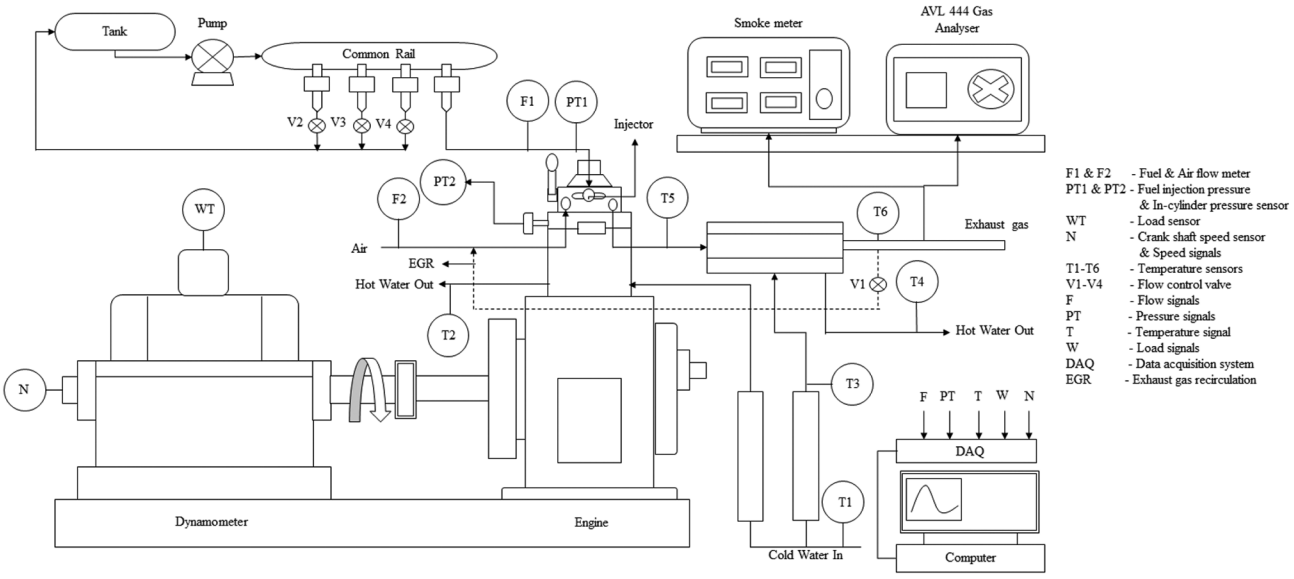

Fig. 2 — Sample test fuel blend EPMD85 and ULSD

the engine speed and the crankshaft angle. The optical encoder, pressure transducer, temperature sensor (Radix K-type), and flow rate signal were connected to data acquisition system (DAQ-NI USB-6210). Using a USB connection, this DAQ was linked to the computer. This analysis software was used to evaluate the performance, such as brake power (BP), brake thermal efficiency (BTE), brake mean effective pressure (BMEP), specific fuel consumption (SFC), in-cylinder pressure and heat release rate (HRR). Engine exhaust emissions, including UBHC, CO, CO_2, O_2 and NO_x, were measured using the AVL 444 gas analyzer. Additionally, the intensity of smoke produced by the test engine was measured with the AVL 473C smoke meter.

Table 2 — Technical specification of engine test rig.

Engine Operation Parameters	Specifications
Engine Model	Make Kirloskar, Type vertical single cylinder, 4 stroke, Diesel fuel, water cooled
Swept Volume (cc)	661.45
Engine Bore/Stroke (mm)	87.5/110
Compression ratio	17.5:1
Rated brake power (kW)	4.5 at 1800 rpm
Ignition system	Compression ignition system
Fuel injection system	Direct Injection (Drive solenoid driven)
High pressure system	CRDI
Fuel injection pressure (bar)	600-1400
Electronic control unit	Model Nira i7r
Number of valves	2 Valves (1 Inlet. 1 Outlet)
Interfacing Software	"Engine soft" Engine performance analysis software

Engine modifications

According to the literature review, the development of a bio-ethanol (EPMD85) fuelled CRDI diesel engine requires modification to the combustion chamber geometry[36-38], fuel injection pressure[39,40,47,48] and compression ratio[41,48] as these factors significantly influence engine performance and emission. In a direct-injected CI engine, the combustion chamber geometry enhancing swirl intensity and injection pressure influences air-fuel mixing. This study examined different combustion chamber designs, including standard hemispherical combustion chamber (ULSD-HCC) and modified hemispherical combustion chamber (EPMD85-HCC) and toroidal re-entrant combustion chamber (EPMD85-TRCC) as shown in Fig. 3. The test fuel (EPMD85) has a high heat of vaporization, demands greater in-cylinder temperature to achieve complete evaporation. To enhancing performance and lower emission, the standard geometry HCC (CR-17.5:1) for

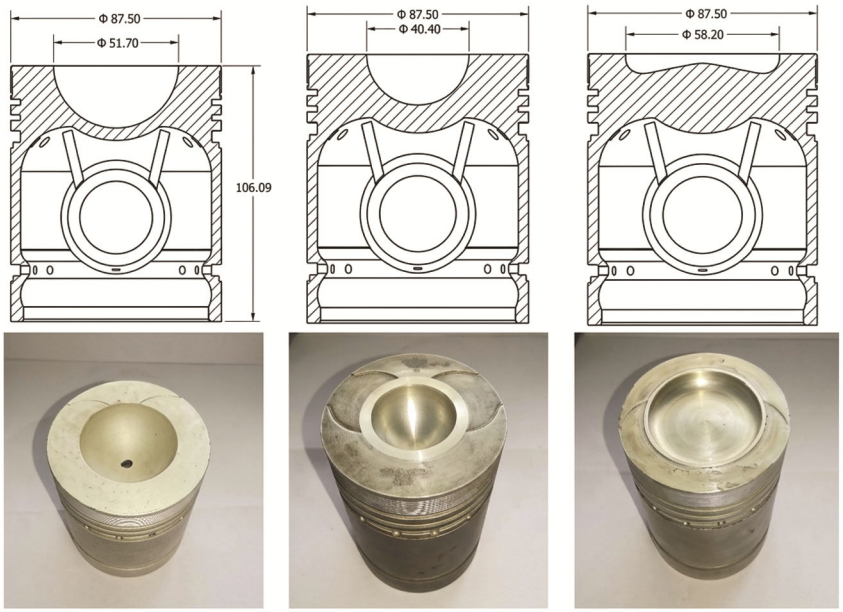

Fig. 3 — Schematic diagram of engine test rig

ULSD was replaced with newer geometries HCC (CR-28.5:1) and TRCC (CR-28.5:1) for EPMD85. The compression ratio of the EPMD85 fueled engine was increased from 17.5:1 to 28.5:1 by varying the bowl volume in both combustion chamber configurations for shorter ignition delay period[41]. Bapu *et al*.[42] reported that re-entrant combustion chambers enhance combustion by increasing in-cylinder turbulence and flow velocity. Higher injection pressure reduce fuel droplet size, improves air-fuel mixing and spray characteristics and promotes faster combustion and deeper fuel penetration into the air, thereby reducing PM emissions[40,48,49]. The experimental engine was equipped with CRDI injection system, enabling adjustment of the injection pressure from 600 bar to 1400 bar without the need for additional equipment.

Test method

Diesel-RK is a multi-zone thermodynamic engine simulation tool, which was employed to simulate and optimize the in-cylinder processes of a single cylinder CRDI compression ignition engine. It predicts engine characteristics by solving mass and energy equation over the engine cycle[42]. Both experiment and simulation investigation were conducted using ULSD and EPMD85 fuels. The test fuels properties (Table 1) and engine specification (Table 2) were used as input parameter for the Diesel-RK model under the standard operating conditions of a experimental engine, with fuel injection time 23°CA bTDC (Crank angle) (Before Top Dead Center). The simulations were performed by varying injection pressure (IP) from 600 to 1400 bar, compression ratio 28.5:1 and modified three toroidal re-entrant combustion chambers (EPMD85-TRCC-A,B &C) using EPMD85 fuel. The combustion chamber geometrical parameters are presented in Table 3. Based on the simulation results, the TRCC-B geometry and IP of 1200 bar were selected as optimal for EPMD85 fuel, as they provided favorable value of SFC, NO_x, ID, and PM. Experiments were conducted using ULSD with the standard hemispherical chamber under different load conditions to evaluate baseline performance, combustion and emission characteristics at the manufacture recommended injection pressure, injection timing and compression ratio of 220 bar, 23°CA bTDC, and 17.5:1, respectively. These conditions served as reference values for comparison with the modified combustion chamber configuration. Subsequent experiments were performed using EPMD85 fuel with HCC and TRCC-B chambers at an optimized compression ratio of 28.5:1 and injection pressure of 1200 bar, while maintaining the same injection timing as the baseline engine. The present investigation contains the use of various instruments to measure the physical parameters and their accuracy may be influenced by operating conditions, environment and instrument limitations etc. Therefore, an uncertainty analysis considering zero calibration and both fixed and random error was performed and overall uncertainty was calculated using Eq. 2.

$$\Delta U = \sqrt{\left\{\frac{\partial U}{\partial x_1}(\Delta x_1)\right\}^2 + \left\{\frac{\partial U}{\partial x_2}(\Delta x_2)\right\}^2 + \cdots + \left\{\frac{\partial U}{\partial x_n}(\Delta x_n)\right\}^2} \quad \ldots(2)$$

where, ΔU- Measured quantity uncertainty, Δx_1– Independent variable uncertainty, x_1– Self-regulating variable. The overall uncertainty of the experimental performance and emission measurements were found

Table 3 — Geometrical parameter of combustion chambers (Bio-ethanol fuel-EPMD85), CR-28.5:1)

Description	Chamber - A	Chamber - B	Chamber - C
	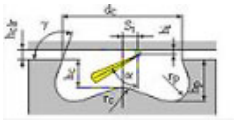	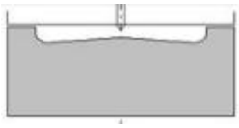	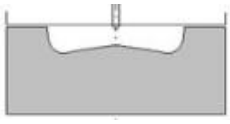
Name of the combustion chamber	EPMD85-TRCC - A	EPMD85-TRCC - B	EPMD85-TRCC – C
External Diameter of the piston bowl, d_c, (mm)	66.2	58.2	55.2
In-center piston bowl depth, h_c, (mm)	4	4	7
Radius of sphere in centre of piston bowl, r_c, (mm)	4	4	7
Depth of combustion chamber in periphery, h_p, (mm)	6.1	8.1	10.1
Radius of hollow chamber in periphery of bowl, r_p, (mm)	4.31	6.31	6.31
Inclination angle of a bowl forming to a plane of the piston crown, gamma, (deg)	101	99	84
Top-clearance at TDC, h_{clr}, (mm)	1.001	1.001	1.001
Swirl ratio	2.3	2.9	3.1

to be ±2% and ±2.2%, respectively. The instrument uncertainty values are presented in Table 4.

Results and Discussion

In the simulation study, three redesigned toroidal re-entrant combustion chambers (TRCC-A, B & C) were examined using the Diesel-RK tool with EPMD85 fuel in terms of SFC, NO_x, PM, and ID. Based on the simulation results, TRCC-B was identified as the optimum configuration and was selected for experimental validation. Consequently, Experimental investigations were subsequently carried out on the baseline ULSD-HCC engine, the modifiedEPMD85-HCC and the optimized EPMD85-TRCC-B engine configurations. The Diesel-RK simulation result of performance, combustion and emission results for these configurations were validated against the corresponding experimental data under identical operating conditions.

Table 4 — Uncertainties in the measurement parameter

Measured Variable	Uncertainty percentage (%)
Speed (rpm)	±1.0%
Load (kg)	±0.7%
Airflow (kg/h)	±1.3%
Fuel flow (kg/h)	±0.7%
Engine Power (kW)	±0.8%
Exhaust temperature (°C)	±0.2%
Cylinder Pressure (bar)	±0.6%
HC (ppm)	±1.2%
NOx (ppm)	±1.3%
CO (% vol.)	±0.6%
CO2 (% vol.)	±0.8%
Smoke (HSU)	±1.0%

Simulation validation of combustion chamber geometry (CR-28.5:1) and Injection pressure on EPMD85 fuel

Variation of specific fuel consumption (SFC) against injection pressure (IP)

Fig. 4 illustrates the impact of IP on SFC across three toroidal re-entrant combustion chambers (TRCC-A, B&C) using EPMD85 fuel under varying cycle fuel mass (CFM). As the IP increases from 600 bar to 1400 bar, SFC consistently declines across all three combustion chambers at 0%, 50% and 100% loading conditions. This reduction is attributed to improved fuel atomization at higher IP, which enhance air-fuel mixture and promotes faster and more complete combustion[50,51]. At an IP of 1200 bar, SFC reaches its minimum at 0% and 50% loading due to optimal spray and mixing characteristics, resulting in more efficient energy conversion. However, at a higher IP of 1400 bar under 0% load conditions, the SFC increases for all chamber configurations. This behaviour can be attributed to an excessively fine fuel atomization combined with insufficient in-cylinder temperature at low load, which adversely affect the evaporation and combustion of EPMD85. The resulting charge cooling leads to improper combustion, thereby increasing fuel consumption for the same energy output. It was also noted that the SFC for TRCC-B chamber is slightly lower than that of TRCC-A&C chambers at all engine loads. The better swirl ratio in TRCC-B, which enhances atomization and air fuel mixing,

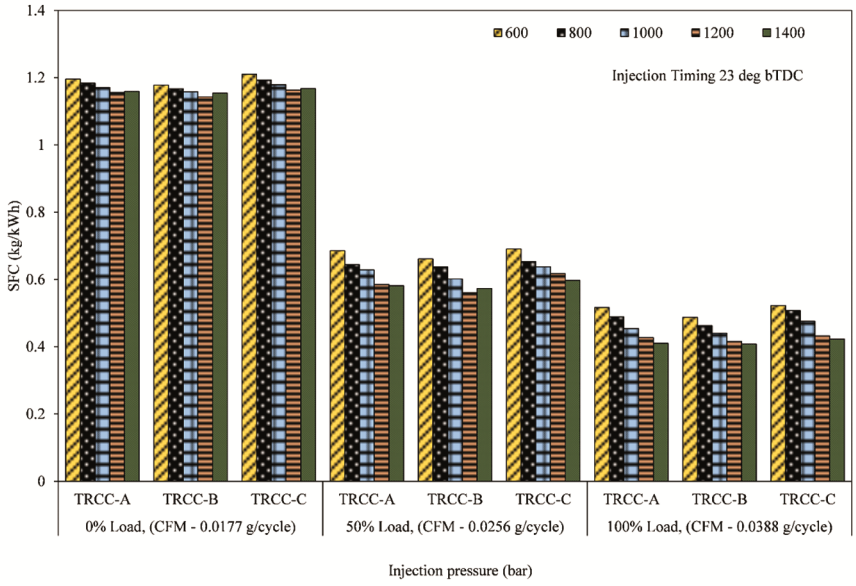

Fig. 4 — Schematic and photographic view of various combustion chamber geometry

may contribute to better combustion of EPMD85 fuel[52,53].

Variation of ignition delay (ID) against (IP)

Fig. 5 depicts the impact of IP on ID for the modified combustion chamber using EPMD85 at different cycle fuel mass (CFM). It was noted that the ID decreases as the IP increases for three modified TRCC engine at 0%, 50% and 100% loading conditions. This may be due to the increasing IP and the high compression ratio (CR-28.5:1).These factors lead to an increase in-cylinder temperature and a decrease in fuel droplet size. Consequently, this increases the efficiency of premixed combustion by enhancing the atomization of the air-fuel mixture. As a result, the duration of the ignition delay time decreases for all combustion chamber geometry as the IP and CR increases[54,55]. In 100% load, the ID increases at 1400 bar IP at all the modified chambers. This may be due to fuel impingement on the cylinder wall, which leads to an increase in the atomization period as a result of incomplete combustion and engine performance. For all loads, the ID for TRCC-B was slightly lower than that of TRCC-A&C. This may be due to the higher in-cylinder wall temperature and homogeneous mixture of EPMD85 and air, resulting from the enhanced air motion in TRCC-B, which improves combustion of the EPMD85 and subsequently reduces the ID[42,56].

Variation of particulate matter (PM) against IP

The effect of IP on PM in a modified combustion chamber using EPMD85 at different cycle fuel mass (CFM) is shown in Fig. 6. Changing IP and bio-

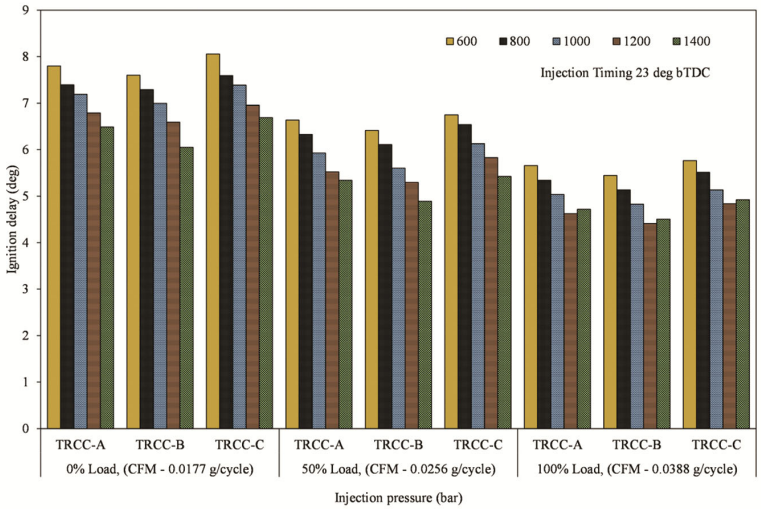

Fig. 5 — Variation of SFC with respect to IP (Load condition - 0%, 50% & 100%)

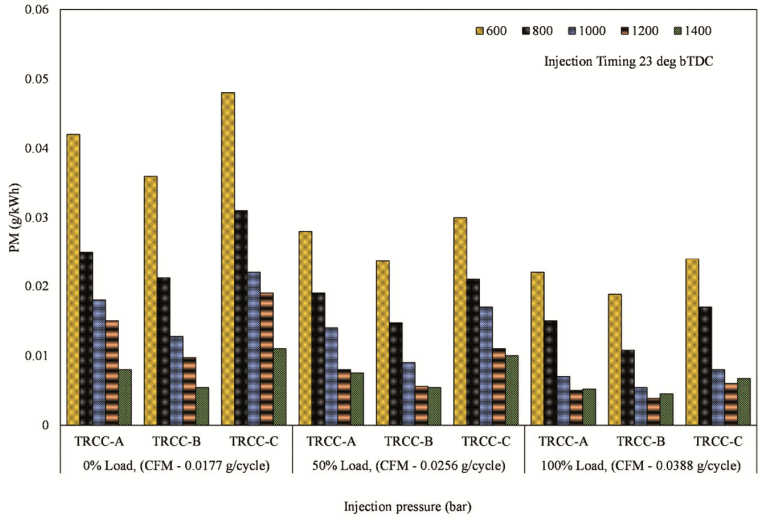

Fig. 6 — Variation of ID with respect to IP (Load condition - 0%, 50% & 100%)

ethanol (EPMD85) are pre-combustion approaches for reducing PM in CI engines. It was noted that the PM decreases as the IP increases in three modified TRCC chambers under 0%, 50%, and 100% loading conditions. This could be attributed to better atomization, a higher compression ratio and the presence of oxygen molecules in EPMD85, which contributed to complete combustion, a higher in-cylinder temperature and reduced formation of PM. Generally, the formation of PM is caused by larger fuel droplets, improper atomization, oxygen deficiency, and excess fuel accumulation. For all combustion chamber geometry, the PM decreased as the IP increased from 600 bar to 1400 bar at 0% and 50% load. In 100% load, the PM increases at 1400 bar IP, this may be attributes to fuel accumulation, which leads to poor atomization and incomplete combustion[57,58]. When using EPMD85, TRCC-B has a lower PM than other TRCC-A&C chambers at all loads. The improved swirl ratio and higher compression ratio in TRCC-B contribute to enhanced air motion, resulting in more efficient combustion of EPMD85. This reduces fuel accumulation and air deficiency, ultimately leading to a decrease in PM emissions. In all load conditions, the TRCC-A&C chambers have a slightly higher compared to the TRCC-B chambers. This may be because of the swirl ratio and combustion chamber depth, which slow down the atomization of the air-fuel mixture[36].

Variation of oxides of nitrogen (NO_x) against IP for various piston bowl geometry

Fig. 7 Illustrate the effect of IP on NO_x emission for the three toroidal re-entrant combustion chambers using EPMD85 with varying CFM. It was found that as the IP increases from 600 bar to 1400 bar, the NOx emission increases for all three combustion chambers at 0%, 50% and 100% loading conditions. This trend can be attributed to the combined effect of higher CR and IP, which increases in-cylinder temperature and pressure, as the result of increasing NOx emissions[36,59,60]. EPMD85 fuel has a higher octane rating and oxygen content, allows for higher temperatures without knocking, which can further contribute to increased NOx emissions[61,62]. TRCC-B chamber exhibits higher NO_x emission than TRCC-A&C at 0% and 50% loads due to shorter ignition delay, uneven temperature distribution and improper flame propagation that lead to less controlled combustion, which increases peak temperatures and subsequently NO_x emissions. At full load, the NO_x emission of the TRCC-B is lower than that of TRCC-A&C. This reduction is attributes to improved air-fuel homogeneity and better fuel vaporization in the TRCC-B chamber, which result in a more uniform temperature distribution and comparatively reduce peak combustion temperature[42,62].

According to the simulation results for the three toroidal re-entrant combustion chamber configurations (TRCC-A, B & C) operated withEPMD85 fuel, the TRCC-B chamber outperformed than TRCC-A and TRCC-C chambers across the investigated IP and CR ranges. Particularly, the TRCC-B chamber achieves lower specific fuel consumption (SFC) at an IP of 1200 bar, indicating more efficient fuel usage. Furthermore, the NO_x, PM, and IDfor the TRCC-B chamber are comparable to or lower than those of the TRCC-A and

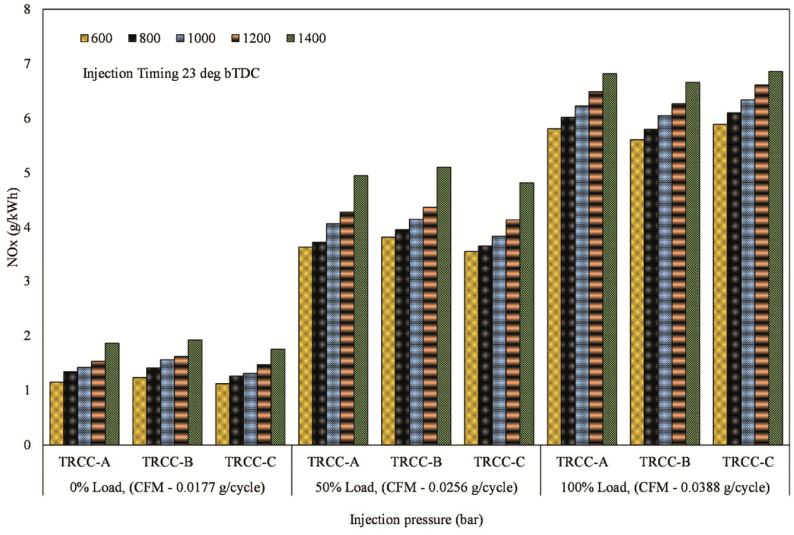

Fig. 7 — Variation of PM with respect to IP (Load condition - 0%, 50% & 100%)

TRCC-C chambers at different loading conditions. At an IP of 1200 bar, the TRCC-B chamber exhibits notable lower PM and shorter ID than the other injection configurations. Overall, the TRCC-B chamber offers a balanced performance profile with improved fuel efficiency and acceptable emissions characteristics, making it the preferred choice among the tested chambers at an injection pressure of 1200 bar.

Simulation and Experimental validation of combustion chamber geometry and IP on EPMD85 and ULSD

Combustion analysis

Fig. 8 illustrates the experiment (EXP) and simulation (SIM) variation of in-cylinder pressure for ULSD and EPMD85 fuel in standard chamber HCC (CR-17.5:1, IP-220 bar) and modified chambers HCC & TRCC-B (CR-28.5:1, IP-1200 bar) across different crank angles, considering varying IP and CR. The experimental peak pressure of ULSD in the standard HCC at 220 bar was 46% and 51% lower than EPMD85 in the HCC and TRCC-B at 1200 bar. This may be due to effective mixing of EPMD85 with air, which is attributed to a decrease in viscosity, a lower flash point and high fuel injection pressure as the result of better combustion. Nevertheless, with EPMD85 operating at an IP of 1200 bar and a CR of 28.5:1, the peak pressure for TRCC-B was 3.5% greater than that for HCC. The toroidal re-entrant combustion chamber and injection pressure enhance air-fuel interaction and fuel vaporization, which could support fuel burning rate and complete combustion. Moreover, EPMD85 fuel has inbuilt oxygen content, which helps for combustion in the TRCC-B chamber. The simulation results align perfectly with the experimental results across all loading conditions. As a result, the modified TRCC-B engine with EPMD85 performed better combustion owing to proper atomization, improved air-fuel mixing and more effective combustion.

Fig. 9 depicts the EXP and SIM heat release rate (HRR) variation with crank angle for standard HCC and modified chambers HCC & TRCC-B using ULSD and EPMD85, respectively. The standard engine operates at IP of 220 bar and CR of 17.5:1, while the modified engine operates at IP of 1200 bar and CR of 28.5:1. It was found experimental that the HRR of EPMD85-TRCC-B and EPMD85-HCC increased by 55% and 44%, respectively, compared to ULSD-HCC. Higher IP and CR, contributed to a more significant HRR during the premixed combustion phase. EPMD85 fuel exhibits higher HRR, owing to its fuel properties like a higher octane rating and viscosity operated at a higher CR, this results in increased in combustion temperature and pressure, ultimately enhancing overall combustion efficiency and further increasing the HRR. The EPMD85-TRCC-B exhibits the highest HRR (135.56 J/deg), followed by EPMD85-HCC (126.52 J/deg) and ULSD-HCC (87.36 J/deg). This is owing to the enhanced air-fuel mixture rate, increased flame propagation, and superior combustion rate.

Performance analysis

Fig. 10 shows the variation of SFC obtained from experimental (EXP) and simulation (SIM) results for the standard HCC (CR-17.5:1, IP-220 bar) with ULSD and modified combustion chamber HCC & TRCC-B(CR-28.5:1, IP-1200 bar) with EPMD85 fuel. From the figure, it is evident that, the modified

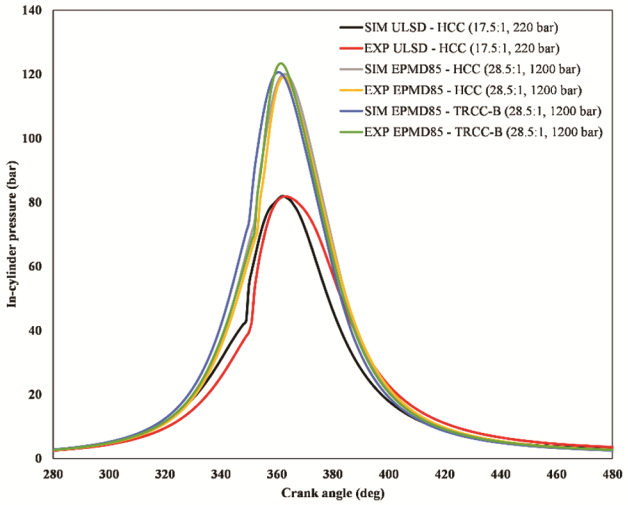

Fig. 8 — Variation of NO_x with respect to IP (Load condition - 0%, 50% & 100%)

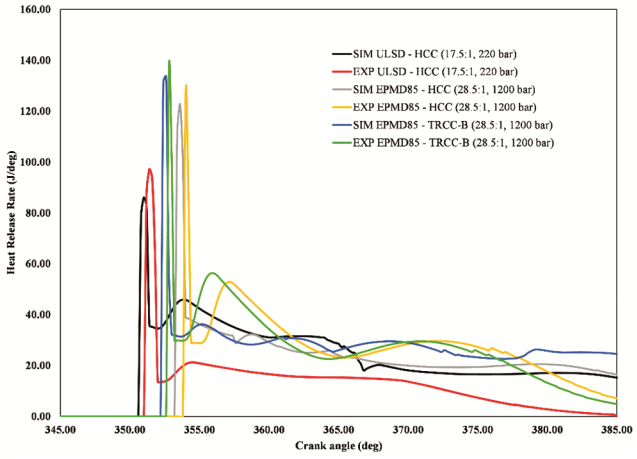

Fig. 9 — Variation of in-cylinder pressure with crank angle (3.42 kW)

combustion chamber (HCC & TRCC-B, CR-28.5:1) with EPMD85 fuel exhibits the highest specific fuel consumption in comparison to the ULSD with standard (HCC, CR-17.5:1) at all loading conditions in both simulation and experimental results. The EPMD85 fuel has a 33% lower calorific value than the ULSD, which causes increase in the SFC characteristics. In experimental results, at 0%, 50% and 100% loads, SFC of EPMD85-HCC & EPMD85-TRCC-B were higher than ULSD-HCC by 43% & 16%, 57% & 49% and 61% & 53%, respectively. The SFC for EPMD85-TRCC-B is lower than EPMD85-HCC by 19%, 5% and 4.5% at 0%, 50% and 100% loading conditions. This improvement is because of enhanced combustion in TRCC-B chamber at higher IP and CR, which facilitates improved air-fuel mixing through finer atomization and better fuel vaporization. In addition, SFC decreases with increasing engine load upto approximately 85% and it starts to increase at higher loads. This may be ascribed to the improved combustion as a result of the increased overall fuel consumption for the same energy output.

Comparison of simulation and experimental result of BTE of standard (HCC, CR-17.5:1) using ULSD and modified combustion chamber (HCC & TRCC-B, CR-28.5:1) using EPMD85 at IP 220 bar and 1200 bar respectively, as shown in Fig. 11. The figure reveals that all results show an increase in BTE as BP increases, and the simulation results closely follow the experimental trend under all loading conditions. BTE of HCC & TRCC-B (CR-28.5:1, IP-1200 bar) with EPMD85 have higher efficiency compared to that of ULSD with standard HCC (CR-17.5:1,

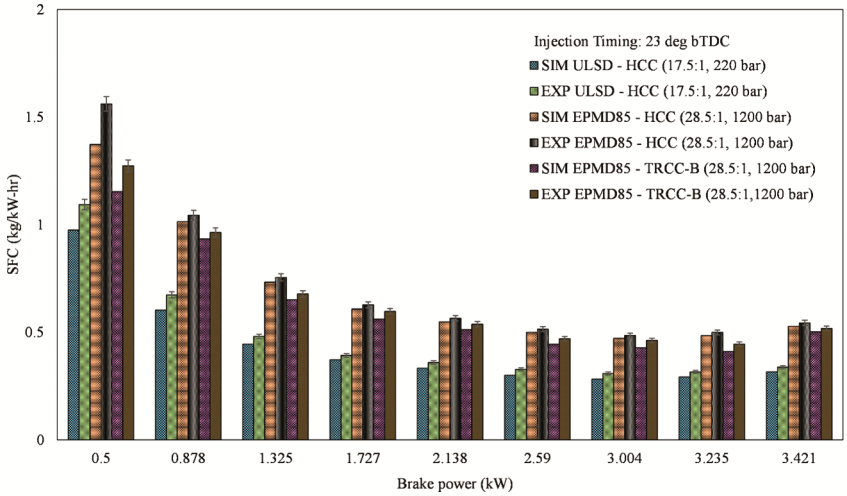

Fig. 10 — Variation of HRR with crank angle (3.42 kW)

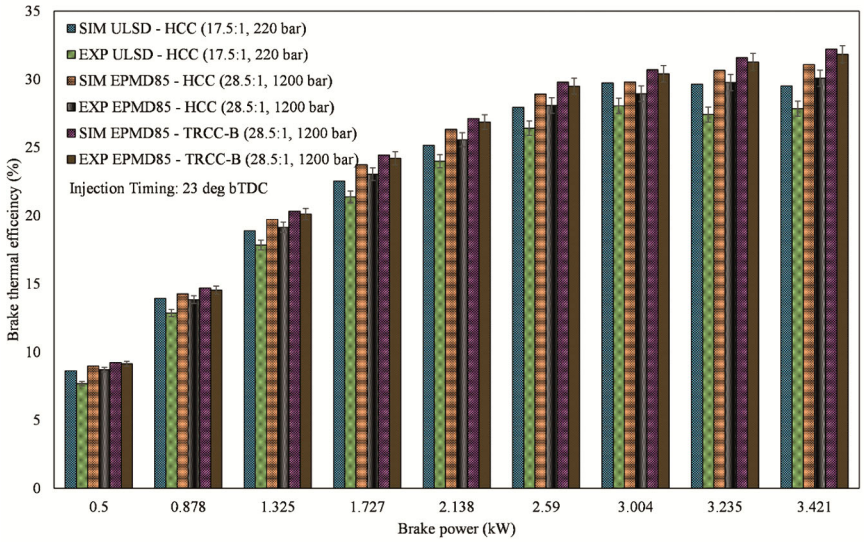

Fig. 11 — Variation of SFC with respect to BP

IP-220 bar) at all conditions. Intrinsic oxygen content, improved atomization and mixing, finer droplets, increased flame spread, and rising temperature and pressure all contribute to faster ignition and rapid combustion in HCC and TRCC-B with EPMD85. In EXP results, at 0%, 50% and 100% loads, BTE of EPMD85-HCC & EPMD85-TRCC-B were higher than ULSD-HCC by 12% & 19%, 7% & 12% and 10% & 14%, respectively. This improvement can be due to increased turbulence of the EPMD85 fuel-air mixture along with enhanced swirl motion, resulting from improved combustion in the TRCC-B chamber. It was observed that BTE increased with higher IP and CR in both the HCC & TRCC-B (CR-28.5:1, IP-1200 bar). This enhancement in BTE may be ascribe to the finer fuel atomization obtained at higher IP and the improved fuel utilization at higher CR.

Emission analysis

Fig. 12 shows the variation of NO_x emission for SIM and EXP results of standard (HCC, CR-17.5:1) with ULSD and modified combustion chamber (HCC & TRCC-B, CR-28.5:1) with EPMD85 fuel at injection pressure 220 bar and 1200 bar, respectively. In a CI engine, the formation of NO_x is owing to excess air present in the combustion chamber, which boosts the combustion rate and increases the in-cylinder temperature above 1500℃, as a result, the nitrogen and oxygen molecules react to form NO_x emission. The SIM and EXP results exhibit strong agreement at all loads. HCC (CR-17.5:1, IP-220 bar) with ULSD formed higher NO_x emission than the HCC & TRCC-B (CR-28.5:1, IP-1200 bar) with EPMD85. The high latent heat of vaporization of EPMD85 results in low combustion temperatures, thereby reducing in-cylinder temperatures and NOx formation. The ability of EPMD85 to tolerate high CR and IP, as well as advance IT (23° bTDC), aids in controlling the combustion temperature and reducing NOx. In EXP results, at 0%, 50% and 100% loads, NO_x of EPMD85-HCC & EPMD85-TRCC-B were lower than ULSD-HCC by 19% & 21%, 11% & 15% and 6% & 8%, respectively. The NO_x for EPMD85-TRCC-B is lower than EPMD85-HCC by 2%, 4% and 2% at 0%, 50% and 100% loading conditions. This can be due to improve air-fuel mixing with TRCC-B and EPMD85, which promotes more uniform combustion, resulting in lower peak temperatures and reduced NO_x formation.

Fig. 13 illustrate the impact on CO emission as a function of brake power (BP) for ULSD in standard HCC (CR-17.5:1, IP-1200 bar) and EPMD85 in modified combustion chamber HCC & TRCC-B (Cr-28.5:1, IP-1200 bar).Overall, ULSD exhibits the highest CO emissions compared to EPMD85. This is due to absence of oxygen in hydrocarbon fuels, which leads to incomplete combustion. The CO emission decreases with increasing load from 0.5 kW to 2.59 kW and it increases from 3.004 kW to 3.412 kW. At full load condition, CO emission increase due to the improper air-fuel mixture, incomplete combustion and insufficient oxygen supply to the combustion chamber. It is observed that, EXP EPMD85-TRCC-B (28.5:1, 1200 bar) 17% and 46% decreased significantly when compared with those of EXP EPMD85-HCC (28.5:1, 1200 bar) and EXP ULSD-

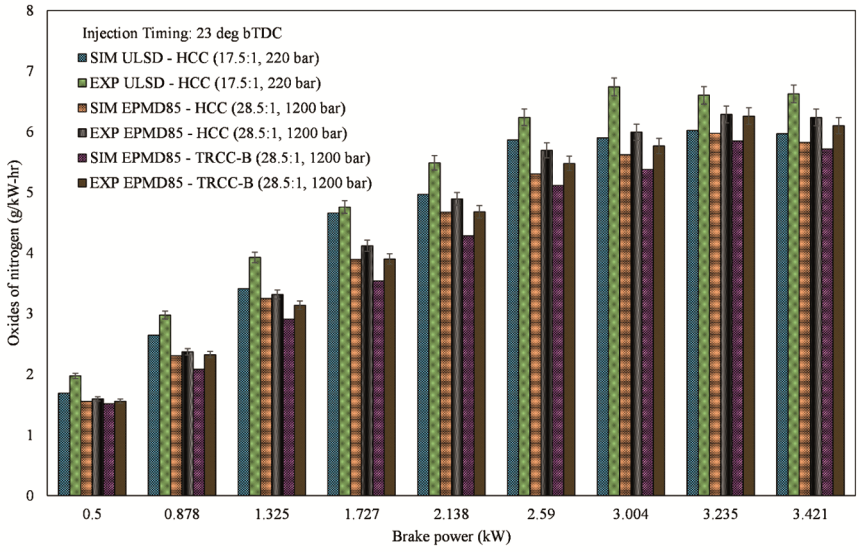

Fig. 12 — Variation of BTE with respect to BP

HCC (17.5:1, 220 bar) at higher load condition. Hence, the influence of higher IP & CR helps to reduce fuel droplet size and increase fuel spray penetration and in-cylinder temperature, leading to better combustion. In the EXP result, at 0%, 50% and 100% loads, CO of EPMD85-HCC & EPMD85-TRCC-B were lower than ULSD-HCC by 5% & 19%, 11% & 34% and 36% & 47% respectively. The CO emission of the EPMD85-TRCC-B is lower than that of theEPMD85-HCC across all loading conditions. This reduction is ascribe to enhanced air-fuel mixing and increase in-cylinder turbulence promoted by the TRCC-B geometry using EPMD85 fuel, which facilitates more complete oxidation of carbon monoxide during combustion.

Fig. 14 illustrates the comparison of UBHC emissions for all of the chambers with ULSD and EPMD85 at varying injection pressures and compression ratios. The modified combustion chamber HCC &TRCC-B (CR-28.5:1, IP-1200 bar) with EPMD85 reduced UBHC emissions over the all load range when compared to the standard HCC (CR-17.5:1, IP-220 bar) with ULSD operation. It has been observed that the EPMD85-TRCC-B geometry emits a lower amount of UBHC compared to the ULSD-HCC and EPMD85- HCC geometry. This may be owing to enhanced combustion of EPMD85, resulting from better swirl and squish motion of air-fuel in TRCC and the presences of high oxygen content in EPMD85. In the EXP result, comparison of ULSD

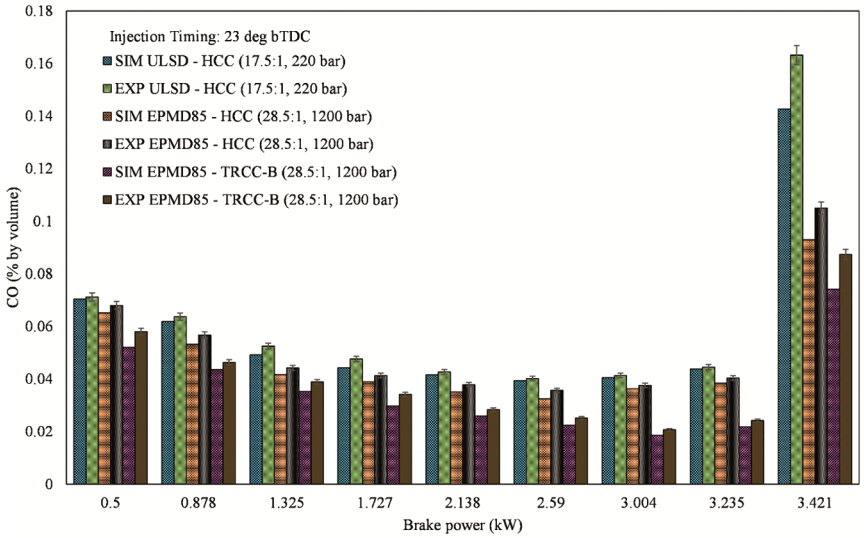

Fig. 13 — Variation of NO_x with respect to BP

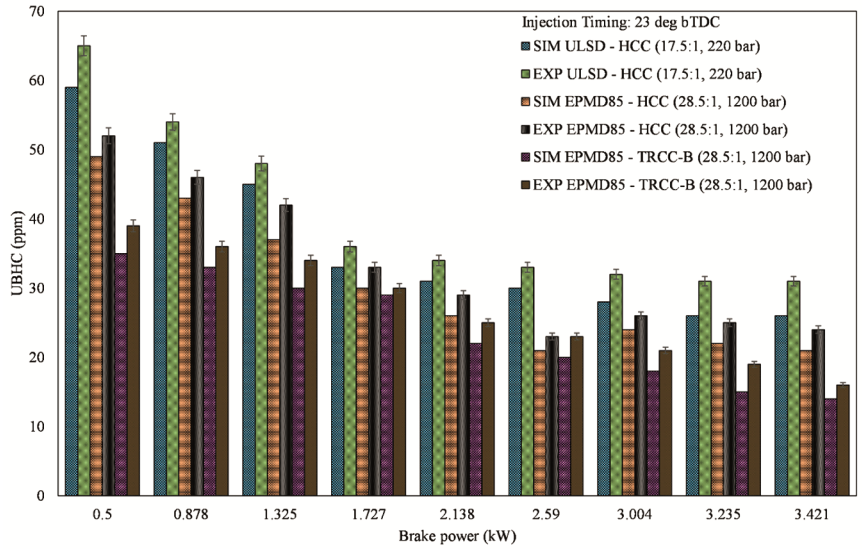

Fig. 14 — Variation of CO with respect to BP

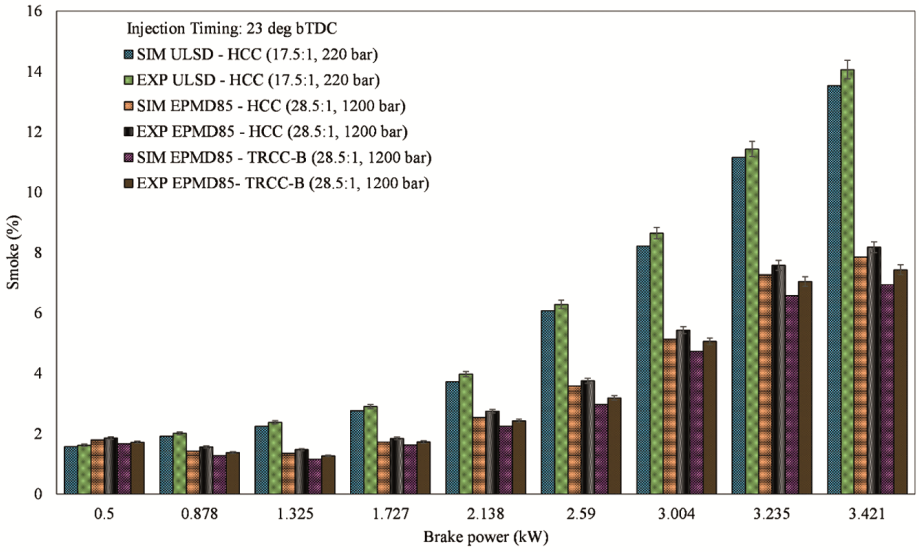

Fig. 15 — Variation of UBHC with respect to BP

HCC (17.5:1, 220 bar) to EPMD85 HCC&TRCC-B (28.5:1, 1200 bar) lowers the UBHC in the range of8% - 27% and 17% - 48% at all the engine loads respectively. The UBHC for EPMD85-TRCC-B is lower than EPMD85-HCC in the range of4% - 33% at all the engine loads. The UBHC emissions increased slightly at 75% loading condition, which may be attributed to improper mixing of the air-fuel mixture. It has been observed that increasing IP and CR with EPMD85 fuel leads to a reduction in the formation of UBHC compared to ULSD. This reduction is attribute to smaller fuel droplet sizes and higher in-cylinder temperature, which enhance atomization, evaporation and complete combustion.

Fig. 15 displays the variation of smoke for ULSD in standard HCC (CR-17.5:1, IP-1200 bar) and EPMD85 in modified combustion chamber HCC & TRCC-B (CR-28.5:1, IP-1200 bar) with respect to engine loads. The formation of smoke due to fuel rich zones, high viscous fuel and high carbon content fuel leads to incomplete combustion, followed by increasing smoke emission. In the EXP result, at 0% load, the smoke of EPMD85-HCC and EPMD85-TRCC-B were higher than that of ULSD-HCC by 15% and 6% respectively. This may be influenced by EPMD85 fuel having a higher heat of vaporization and a lower in-cylinder temperature, which leads to an increase in atomization time, as the result of improper combustion. At 50% and 100% loads, EPMD85-HCC & EPMD85-TRCC-B were lower than ULSD-HCC by 31% & 39 and 42% & 47%, respectively. The reduction in smoke emission can be attribute to the lower carbon and higher oxygen content in EPMD85 fuel. In addition higher IP enhances fuel atomization, a higher CR improves combustion efficiency and the TRCC design promotes better air-fuel mixing while minimizing the formation of hot spots in the combustion chamber.

Fig. 16 presents the variation of CO_2 emission with engine load based on experimental and simulation results for ULSD and EPMD85 fuelled engine configurations. For all fuel and combustion chamber configurations, CO_2 emission increases when increasing engine load due to higher fuel consumption and more complete combustion at elevated in-cylinder temperature. In the EXP result, HCC (CR-17.5:1, IP-220 bar) with ULSD formed higher CO_2 emission than HCC and TRCC-B (CR-28.5:1, IP-1200 bar) with EPMD85. Higher IP & CR improved atomization of the air-fuel mixture and thermal efficiency, as the result of a more complete combustion process, which indirectly affectsCO_2 emission. But, EPMD85 fuel has lower carbon content than ULSD fuel. This is attributed to bio-ethanol a cleaner alternative and it partial carbon neutrality, which leads to producing less CO_2 emission per unit of energy. In the EXP result, at 0%, 50% and 100% loads, CO_2 emission of EPMD85-HCC & EPMD85-TRCC-B were lower than ULSD-HCC by 28% & 37%, 26% & 37% and 22% & 38%, respectively. This is mainly due to enhanced air-fuel mixing with TRCC-B and EPMD85, which promoted more carbon-neutral fuel compared to ULSD and reduced CO_2 formation.

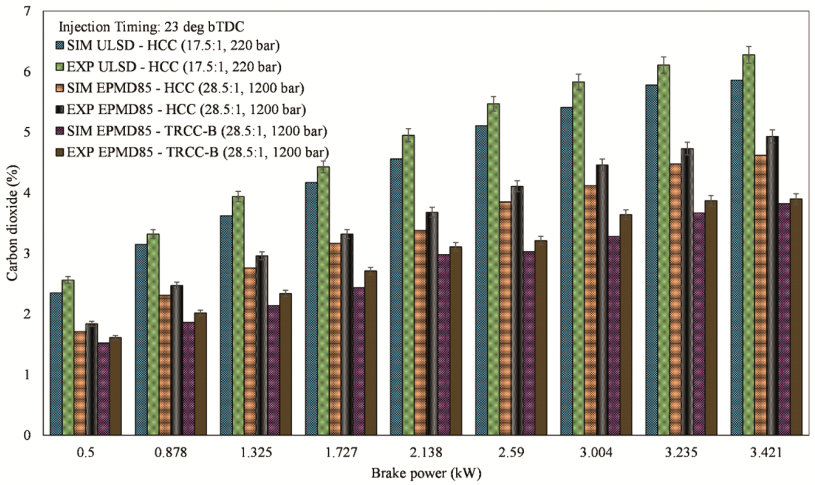

Fig. 16 — Variation of smoke with respect to BP

Conclusion

The present experimental and simulation study examined the impact of combustion chamber geometry and injection pressure on the performance, combustion and emission characteristics of a CRDI diesel engine fuelled with bio-ethanol blend (EPMD85). After blending bio-ethanol with additives, the kinematic viscosity of EPMD85 was observed to be significantly higher than that of ULSD, whereas its calorific value was lower. From the performance perspective, the EPMD85-TRCC-B configuration exhibited higher brake thermal efficiency than both the EPMD85-HCC and ULSD-HCC configurations. However, the modified EPMD85-HCC and TRCC-B chambers unveiled higher specific fuel consumption than ULSD-HCC. This increase in fuel consumption was primarily attributed to the lower energy density of the bio-ethanol blend, which required a higher fuel quantity for the same energy output, despite improved fuel atomization at higher injection pressure and enhanced thermal efficiency at higher compression ratio. On the other hand, when the engine operated with EPMD85 fuel, emissions such as CO, CO_2, NO_X, UBHC and smoke were reduced in the TRCC-B chamber compared to the EPMD85-HCC and ULSD-HCC chambers. This reduction was due to improved combustion of fuel in TRCC-B geometry and the inherent properties of the oxygenated bio-ethanol blend. Overall, the study confirms that theEPMD85-TRCC-B chamber at an injection pressure of 1200 bar and a compression ratio 28.5:1 provides a favorable balance between better engine performance and lower emission, making it a suitable configuration for the efficient utilization of high-percentage bio-ethanol blends in CRDI diesel engine.

Acknowledgement

The authors would like to acknowledge Dr. Mahalingam College of Engineering and Technology, Pollachi, Bannari Amman Institute of Technology, Erode and Coimbatore Institute of Technology, Coimbatore for permitting to use lab facilities.

Conflict of Interest

The authors declare no conflict of interest.

Reference

1 Zheng X, Wu Y, Zhang S, He L & Hao J, Evaluating real-world emissions of light-duty gasoline vehicles with deactivated three-way catalyst converters, *Atmos Pollut Res*, 9 (2018) 126.

2 Tiwari S, Thomas A, Rao P, Chate D M, Soni V K, Singh S, Ghude S D, Singh D & Hopke P K, Pollution concentrations in Delhi India during winter 2015–16: A case study of an odd-even vehicle strategy, *Atmos Pollut Res*, 9 (2018) 1137.

3 Demirbas A, Progress and recent trends in biofuels, *Prog Energy Combust Sci*, 33 (2007) 1.

4 Demirbas A, Importance of biodiesel as transportation fuel, *Energy Policy*, 35 (2007) 4661.

5 Demirbas A, Progress and recent trends in biodiesel fuels, *Energy Convers Manag*, 50 (2009) 14.

6 Awad O I, Mamat R, Ali O M, Sidik N A C, Yusaf T, Kadirgama K & Kettner M, Alcohol and ether as alternative fuels in spark ignition engine: A review, *Renew Sustain Energy Rev*, 82 (2018) 2586.

7 Venu H, Raju V D & Subramani L, Combined effect of influence of nano additives, combustion chamber geometry and injection timing in a DI diesel engine fuelled with ternary (diesel-biodiesel-ethanol) blends, *Energy*, 174 (2019) 386.

8 Silitonga A S, Masjuki H H, Ong H C, Sebayang A H, Dharma S, Kusumo F, Siswantoro J, Milano J, Daud K, Mahlia T M & Chen W H, Evaluation of the engine performance and exhaust emissions of biodiesel-bioethanol-diesel blends using kernel-based extreme learning machine, *Energy*, 159 (2018) 1075.

9 Agarwal A K, Biofuels (alcohols and biodiesel) applications as fuels for internal combustion engines, *Prog Energy Combust Sci*, 33 (2007) 233.

10 Giakoumis E G, Rakopoulos C D, Dimaratos A M & Rakopoulos D C, Exhaust emissions with ethanol or n-butanol diesel fuel blends during transient operation: A review, *Renew Sustain Energy Rev*, 17 (2013) 170.

11 Sakthivel P, Subramanian K A & Mathai R, Indian scenario of ethanol fuel and its utilization in automotive transportation sector, *Resour Conserv Recycl*, 132 (2018) 102.

12 Shen L, Lei J & Bi Y, Performance and emission characteristics of diesel engine fueled with ethanol-diesel blends in different altitude regions, *J Biomed Biotechnol*, 1 (2011) 417.

13 Gerdes K R & Suppes G J, Miscibility of ethanol in diesel fuels, *Ind Eng Chem Res*, 40 (2001) 949.

14 Jaichandar S & Annamalai K, Combined impact of injection pressure and combustion chamber geometry on the performance of a biodiesel fueled diesel engine, *Energy*, 55 (2013) 330.

15 Ibrahim A, Investigating the effect of using diethyl ether as a fuel additive on diesel engine performance and combustion, *Appl Therm Eng*, 107 (2016) 853.

16 De-Caro P S, Mouloungui Z, Vaitilingom G & Berge J C, Interest of combining an additive with diesel-ethanol blends for use in diesel engines, *Fuel*, 80 (2001) 565.

17 Tutak W, Bioethanol E85 as a fuel for dual fuel diesel engine, *Energy Convers Manag*, 86 (2014) 39.

18 Bhale P V, Deshpande N V & Thombre S B, Improving the low temperature properties of biodiesel fuel, *Renew Energy*, 34 (2009) 794.

19 Hansen A C, Zhang Q & Lyne P W L, Ethanol-diesel fuel blends-A review, *Bioresour Technol*, 96 (2005) 277.

20 Turkcan A, Effects of high bioethanol proportion in the biodiesel-diesel blends in a CRDI engine, *Fuel*, 223 (2018) 53.

21 Guo L, Yan Y Y, Tan M, Li H & Peng Y, An experimental study on improving the ignition of ethanol-diesel blended fuel (EDBF), *Chem Eng Commun*,198 (2011) 1263.

22 Patil A R & Taji S G, Effect of oxygenated fuel additive on diesel engine performance and emission: A review, *J Mech Civil Eng*, 3 (2003) 30.

23 Saravanakumar L, Bapu B R R & Prasad B D, Performance and emission characteristics of a CI engine operating on methyl esters blended diesel with di-methyl carbonate additives, *Int Energy J*, 14 (2014) 121.

24 Jawre S S, Diethyl ether as additive and its effect on diesel engine performance: A review, *GRD J Eng*, 1 (2016) 27.

25 Simonsen H & Chomiak J, Testing and evaluation of ignition improvers for ethanol in a DI diesel engine, *SAE Tech Pap*, 104 (1995) 1861.

26 Rakopoulos D C, Rakopoulos C D & Giakoumis E G, Impact of properties of vegetable oil, bio-diesel, ethanol and n-butanol on the combustion and emissions of turbocharged HDDI diesel engine operating under steady and transient conditions, *Fuel*, 156 (2015) 1.

27 Rakopoulos D C, Rakopoulos C D, Giakoumis E G, Papagiannakis R G & Kyritsis D C, Influence of properties of various common bio-fuels on the combustion and emission characteristics of high-speed DI (direct injection) diesel engine: Vegetable oil, bio-diesel, ethanol, n-butanol, diethyl ether, *Energy*, 73 (2014) 354.

28 Rakopoulos D C, Rakopoulos C D, Giakoumis E G & Dimaratos A M, Characteristics of performance and emissions in high-speed direct injection diesel engine fueled with diethyl ether/diesel fuel blends, *Energy*, 43 (2012) 214.

29 Rakopoulos D C, Rakopoulos C D, Giakoumis E G & Dimaratos A M, Studying combustion and cyclic irregularity of diethyl ether as supplement fuel in diesel engine, *Fuel*, 109 (2013) 325.

30 Bailey B, Eberhardt J, Goguen S & Erwin J, Diethyl ether (DEE) as a renewable diesel fuel, *SAE Tech Pap*, 106 (1997) 1578.

31 Venu H & Madhavan V, Influence of diethyl ether (DEE) addition in ethanol-biodiesel-diesel (EBD) and methanol-biodiesel-diesel (MBD) blends in a diesel engine, *Fuel*, 189 (2017) 377.

32 Roy M M, Investigation of methyl tertiary butyl ether-diesel combustion and odorous emissions in a direct-injection diesel engine, *Proc Inst Mech Eng Part D: J Autom Eng*, 222 (2008) 251.

33 Sivakumar V, Sarangan J & Anand R B, Performance, combustion and emission characteristics of a CI engine using MTBE blended diesel fuel, *Proc Int Conf Front Autom Mech Eng*, (2010) 170.

34 Gjirja S, Olsson E & Karlström A, Considerations on engine design and fuelling technique effects on qualitative combustion in alcohol diesel engines, *SAE Tech Pap*, (1998) 1.

35 Premnath S & Devaradjane G, Improving the performance and emission characteristics of a single cylinder diesel engine having reentrant combustion chamber using diesel and Jatropha methyl esters, *Ecotoxicol Environ Saf*, 121 (2015) 10.

36 Gafoor C P A & Gupta R, Numerical investigation of piston bowl geometry and swirl ratio on emission from diesel engines, *Energy Convers Manag*, 101 (2015) 541.

37 Mamilla V R, Mallikarjun M V & Rao G L N, Effect of combustion chamber design on a DI diesel engine fuelled with jatropha methyl esters blends with diesel, *Proc Eng*, 64 (2013) 479.

38 Jaichandar S & Annamalai K, Effects of open combustion chamber geometries on the performance of pongamia biodiesel in a DI diesel engine, *Fuel*, 98 (2012) 272.

39 Sayin C, Ozsezen A N & Canakci M, The influence of operating parameters on the performance and emissions of a DI diesel engine using methanol-blended-diesel fuel, *Fuel*, 89 (2010) 1407

40 Jiaqiang E, Pham M, Deng Y, Nguyen T, Duy V, Le D, Zuo W, Peng Q & Zhang Z, Effects of injection timing and injection pressure on performance and exhaust emissions of a common rail diesel engine fueled by various concentrations of fish-oil biodiesel blends, *Energy*, 149 (2018) 979.

41 Raheman H & Ghadge S V, Performance of diesel engine with biodiesel at varying compression ratio and ignition timing, *Fuel*, 87 (2008) 2659.

42 Bapu B R R, Saravanakumar L & Prasad B D, Effects of combustion chamber geometry on combustion characteristics of a DI diesel engine fueled with calophyllum inophyllum methyl ester, J Energy Inst, 90 (2017) 82.

43 Choi C Y & Reitz R D, Experimental study on the effects of oxygenated fuel blends and multiple injection strategies on DI diesel engine emissions, *Fuel*, 78 (1999) 1303.

44 Li R, Wang Z, Ni P, Zhao Y, Li M & Li L, Effects of cetane number improvers on the performance of diesel engine fuelled with methanol/biodiesel blend, *Fuel*, 128 (2014) 180.

45 Li D G, Zhen H, Xingcai L, Wu-Gao Z & Jian-Guang Y, Physico-chemical properties of ethanol-diesel blend fuel and its effect on performance and emissions of diesel engines, *Renew Energy*, 30 (2005) 967.
46 Abu-Qudais M, Haddad O & Qudaisat M, Effect of alcohol fumigation on diesel engine performance and emissions, *Energy Conver Manag*, 41 (2000) 389.
47 Hountalas D T, Kouremenos D A, Binder K B, Schwarz V & Mavropoulos G C, Effect of injection pressure on the performance and exhaust emissions of a heavy duty DI diesel engine, *SAE Tech Pap*, (2003) 1.
48 Jindal S, Nandwana B P, Rathore N S & Vashistha V, Experimental investigation of the effect of compression ratio and injection pressure in a direct injection diesel engine running on Jatropha methyl ester, *Appl Therm Eng*, 30 (2010) 442.
49 Kumar S, Dinesha P & Rosen M A, Effect of injection pressure on the combustion, performance and emission characteristics of a biodiesel engine with cerium oxide nanoparticle additive, *Energy*, 185 (2019) 1163.
50 Emiroğlu A O, Effect of fuel injection pressure on the characteristics of single cylinder diesel engine powered by butanol-diesel blend, *Fuel*, 256 (2019) 115928.
51 Mohan B, Yang W & Chou S K, Fuel injection strategies for performance improvement and emissions reduction in compression ignition engines-A review, *Renew Sustain Energy Rev*, 28 (2013) 664.
52 Zhou H, Li X, Zhao W & Liu F, Effects of separated swirl combustion chamber geometries on the combustion and emission characteristics of DI diesel engines, *Fuel*, 253 (2019) 488.
53 Chen Y, Li X, Shi S, Zhao Q, Liu D, Chang J & Liu F, Effects of intake swirl on the fuel/air mixing and combustion performance in a lateral swirl combustion system for direct injection diesel engines, *Fuel*, 286 (2021) 119376.
Du W, Zhang Q, Zhang Z, Lou J & Bao W, Effects of injection pressure on ignition and combustion characteristics of impinging diesel spray, *Appl Energy*, 226 (2018) 1163.
54 Liu J, Yao A & Yao C, Effects of diesel injection pressure on the performance and emissions of a HD common-rail diesel engine fueled with diesel/methanol dual fuel, *Fuel*, 140 (2015) 192.
55 Shahabuddin M, Liaquat A M, Masjuki H H, Kalam M A & Mofijur M, Ignition delay, combustion and emission characteristics of diesel engine fueled with biodiesel, *Renew Sustain Energy Rev*, 21 (2013) 623.
56 Cho J, Si W, Jang W, Jin D, Myung C L & Park S, Impact of intermediate ethanol blends on particulate matter emission from a spark ignition direct injection (SIDI) engine, *Appl Energy*, 160 (2015) 592.
57 Sakai S & Rothamer D, Impact of ethanol blending on particulate emissions from a spark-ignition direct-injection engine, *Fuel*, 236 (2019) 1548.
58 Ye P & Boehman A L, An investigation of the impact of injection strategy and biodiesel on engine NOx and particulate matter emissions with a common-rail turbocharged di diesel engine, *Fuel*, 97 (2012) 476.
59 Cao D N, Hoang A T, Luu H Q, Bui V G & Tran T T H, Effects of injection pressure on the NOx and PM emission control of diesel engine: A review under the aspect of PCCI combustion condition, *Energy Sources Part A: Recov Util Environ Eff*, 1 (2020) 7414.
60 Gnanamoorthi V & Devaradjane G, Effect of compression ratio on the performance, combustion and emission of di diesel engine fueled with ethanol-Diesel blend, *J Energy Inst*, 88 (2015) 19.
62 Balasubramanian R & Subramanian K A, Experimental investigation on the effects of compression ratio on performance, emissions and combustion characteristics of a biodiesel-fueled automotive diesel engine, *Biofuels*, 12 (2021) 913.